

DOI 10.17816/transsyst20184230-44

© S. Mu, J. Kang, S. Wang, Y. Liu, C. He

Tongji University
(Shanghai, China)

A METHOD OF THRUST RIPPLE SUPPRESSION FOR LONG STATOR LINEAR SYNCHRONOUS MOTOR

Abstract. With the advantages of high speed, low noise and high efficiency, the electromagnetic suspension (EMS) type maglev train has a good prospect in railway transportation. It is based on the long stator linear synchronous motor (LSLSM). However, due to cogging effect, end effect and the harmonics in the stator current and flux density distribution around the air-gap, the thrust generated by the LSLSM fluctuates. The thrust ripple brings noise, drop of control accuracy, even causes the resonance of train. In this paper, the thrust ripple produced by the cogging effect and flux linkage harmonics is analyzed. Then a method of harmonic current injection is proposed to compensate cogging force and reduce the thrust ripple, without influence the decoupling control of traction and suspension system. The injected current harmonics are controlled under multiple rotating reference frames independently. Finally, based on voltage equations of harmonics, the decoupled harmonic current controllers with harmonic voltage feedforward are designed, which improve the performance of current harmonics response and thrust ripple suppression. Simulation results on Simulink verify the effectiveness of proposed thrust ripple suppression method for LSLSM.

Keywords: Maglev, Long stator linear synchronous motor, Thrust ripple, Cogging force, Harmonic current injection, Multiple rotating reference frames, Voltage feedforward

INTRODUCTION

Without contact between vehicle and railway, maglev train is a one of the best options for future high-speed ground transportation system. The electromagnetic suspension (EMS) type maglev transportation system is one representative, and has been applied in the first commercial operation maglev line of world built in Shanghai. It shows advantages of high speed, low noise and high efficiency. The traction of vehicle is based on the long stator linear synchronous motor (LSLSM), where the railway is motor's long stator and the vehicle is the mover.

However, it suffers from the propulsion force fluctuation in operation, which brings noise, deteriorates control accuracy, even causes resonance of vehicle, makes passengers uncomfortable. Generally speaking, nonideal factors in practical LSLSM drive system are main reasons of thrust ripple, such as non-sinusoidal stator currents [1], cogging effect, end effect [2], harmonics of flux linkage, etc.

A lot of research works have been carried out to reduce the thrust ripple of LSM both from motor design and control algorithm. Many methods are

proposed on motor design and reduce thrust ripple by optimizing the structure, including magnet skewing or slot skewing, optimizing pole-arc coefficients [3], auxiliary pole [4] and unequal pole pitch of the stator and mover [5], etc. But the structure optimizing is not a universal method for all the LSM, and hard to eliminate all thrust harmonics.

Other researchers focus on the control strategies to suppress thrust ripple. Some methods to reduce the stator current harmonics by compensating the dead time effect of inverter are proposed [6, 7]. But it can't suppress the main thrust ripple caused by non-sinusoidal distributed magnetic field and cogging force. One way is to obtain the magnitude and phase of thrust ripple and compensate it on the control command. Adaptive algorithm [8], disturbance observer [9], repetitive control [10], iterative learning control [11] are studied since thrust ripple is periodical. Though stator current harmonics will cause electromagnetic force ripple, adequate electromagnetic force harmonics can counteract the reluctance force ripple of motor, which is the essence of suppressing thrust ripple. In [12], harmonic injection is proposed to reduce thrust ripple in linear flux-switching motor. But the harmonic current is controlled by current hysteresis controller, thus the switching frequency is variable. [13] introduces multiple reference frames to solve the bandwidth limits of traditional PI current controller in permanent magnet machines (PMSM). But the coupling of harmonic currents is not considered. In [14], harmonic voltage and current coupling model of PMSM is studied, improves the injection effect of harmonic current and torque ripple reduction performance.

This paper presents a thrust ripple suppression method by harmonic current injection with harmonic voltage feedforward for maglev LSLSM drives. The drive system is based on the rotor flux oriented control (RFOC), and only q -axis current is injected into current harmonics, which won't influence the decoupling of traction and suspension system [15]. Multiple reference frames, harmonic current decoupling and harmonic voltage feedforward are applied in the system, which overcome the bandwidth limits of conventional PI current controller and improve the effect of harmonic current injection and suppression of thrust ripple. The paper starts with introduction of the model of LSLSM, considering cogging force and exciting flux linkage harmonics. Then, thrust ripple suppression method is performed, including determination of proper injected harmonic current and control of reference harmonic current. In the following, simulation results on the LSLSM are presented. The conclusion is given in the end.

THRUST RIPPLE OF LONG STATOR SYNCHRONOUS MOTOR

A. Model of long stator synchronous motor

Assuming symmetry of three phase stator winding and ignoring magnetic saturation, hysteresis, and eddy current, the mathematical model of LMSM in

the rotor flux synchronous rotating coordinates can be written as:

$$\begin{cases} u_d = R_s i_d + L_d \frac{di_d}{dt} - \frac{\pi}{\tau_s} v \psi_q \\ u_q = R_s i_q + L_q \frac{di_q}{dt} + \frac{\pi}{\tau_s} v \psi_d \\ \frac{dv}{dt} = \frac{1}{m} (F_x - F_z) \end{cases} \quad (1)$$

where u_d , u_q , i_d and i_q are the stator voltages and currents on d, q axes, respectively; ψ_d and ψ_q are the stator flux on d, q axes respectively; R_s is total stator resistance; L_d, L_q are the total stator inductance on d, q axes respectively; τ_s is the pole pitch; v is the mover speed; m is the vehicle mass; F_x is the thrust force; F_z is the overall resistance force, consist of air resistance force, magnet resistance force and generator resistance force.

Unlike general rotary motor, the impedance of feed cable, stator section uncovered by vehicle pole and stator section covered by vehicle pole comprise the total stator resistance and inductance of LSLSM [16]. Since the length of stator section is much longer than vehicle length, the leak inductance of stator section uncovered by vehicle makes up the main part of total stator inductance, which leads to inductance L_d approximately equal to L_q .

The stator flux equation on d, q axes is expressed as:

$$\begin{cases} \psi_d = L_d i_d + \psi_{df} \\ \psi_q = L_q i_q + \psi_{qf} \end{cases} \quad (2)$$

where ψ_{df} and ψ_{qf} are the mover exciting flux linkage on d, q axes, produced by excitation winding of vehicle suspension electromagnetic.

The thrust force of LSLSM is composed of electromagnetic force F_e and cogging force F_{cog} , i.e.,

$$F_x = F_e + F_{cog} \quad (3)$$

where F_{cog} is the reluctance force due to slot effect; F_e is produced by the interaction between airgap flux and the stator currents, and equal to the mean value of thrust force. It can be expressed as:

$$F_e = \frac{3\pi}{2\tau_s} (\psi_d i_q - \psi_q i_d) = \frac{3\pi}{2\tau_s} [(\psi_{df} + L_d i_d) i_q - (\psi_{df} + L_d i_q) i_d] \quad (4)$$

Due to decoupling the armature field and excitation field, the rotor field-oriented control (RFOC) and $i_d = 0$ strategy are commonly applied for LSLSM control in practical [15]. In this case, (4) can be simplified as:

$$F_e = \frac{3\pi}{2\tau_s} \psi_{df} i_q \quad (5)$$

B. Flux harmonics

In an ideal LSLSM, where excitation flux is ideal sinusoidal distributed in the air gap, ψ_{qf} is equal to zero and ψ_{df} is constant under RFOC control.

However, because of manufacturing restrictions, there are $6k$ th spatial harmonics in practical in the mover flux linkage in practical, and can be expressed in Fourier series as:

$$\begin{cases} \Psi_{df} = \Psi_{d0} + \sum_{k=1}^{+\infty} \Psi_{d\pm 6k} e^{i\left(\pm 6k \frac{\pi x}{\tau_s}\right)} = \Psi_{d0} + \sum_{k=\pm 1, \pm 2, \pm 3, \dots} \Psi_{d6k} \cos\left(6k \frac{\pi x}{\tau_s}\right) \\ \Psi_{qf} = \Psi_{q0} + \sum_{k=1}^{+\infty} \Psi_{q\pm 6k} e^{i\left(\pm 6k \frac{\pi x}{\tau_s}\right)} = \sum_{k=1, 2, 3, \dots} \Psi_{q6k} \cos\left(6k \frac{\pi x}{\tau_s}\right) \end{cases} \quad (7)$$

where x is the mover position relative to phase A; Ψ_{d6k} and Ψ_{q6k} are the harmonic coefficients of $6k$ th flux harmonic on d, q axes respectively. The dc component of d -axis flux linkage Ψ_{d0} is non-zero, while Ψ_{q0} equals to zero.

According to the thrust equation, the spatial harmonics of flux linkage will result in the $6k$ th periodical thrust ripple of real LSLSM with sinusoidal fed stator currents. Moreover, it brings harmonics in back electromotive force (EMF), and deteriorate the control effect of current controller.

C. Cogging force

The stator windings are placed in the stator slots on LSLSM of maglev. When the mover poles approaching or leaving the stator teeth, the reluctance and magnetic field distribution vary. That leads to the fluctuation of magnetic energy of motor, generating additional reluctance force on mover. The cogging force is independent of the stator current while closely related to mover position. The period of cogging force is the distance between neighboring slots. Since there are six slots at each pole pair, the cogging force fluctuates 6 times within one pair of poles. Fourier expression of cogging force can be written as

$$F_{\text{cog}} = F_{c0} + \sum_{k=1}^{+\infty} F_{c\pm 6k} e^{i\left(\pm 6k \frac{\pi x}{\tau_s}\right)} \quad (8)$$

where F_{c6k} is the harmonic coefficients of $6k$ th component of Fourier series, and the dc component F_{c0} is equal to zero.

HARMONIC CURRENT INJECTION

A. Reference Harmonic Current

Taking Fourier expressions of flux linkage equation (7) and cogging force equation (8) into the thrust expression (3), it yields

$$F_x = \frac{3\pi}{2\tau_s} \left(\sum_{k=0}^{+\infty} \Psi_{d\pm 6k} e^{i\left(\pm 6k \frac{\pi x}{\tau_s}\right)} \right) \cdot i_q + \sum_{k=0}^{+\infty} F_{c\pm 6k} e^{i\left(\pm 6k \frac{\pi x}{\tau_s}\right)} \quad (9)$$

The formula shows that there will be $6k$ th periodical thrust ripple of LSLSM if i_q is kept constant when flux linkage harmonics and cogging force exist. One way to compensate the cogging force and suppress thrust ripple is to inject harmonic current into q -axis current. To generate $6k$ th periodical

electromagnetic force, 6 k th current harmonics are needed. The desired q -axis current can be assumed as

$$i_q^* = i_0 + \sum_{k=1}^{+\infty} i_{\pm 6k} e^{i\left(\pm 6k\pi\theta_e + \frac{\pi}{2}\right)} \quad (10)$$

where i_{6k} are the complex coefficients of 6 k th harmonics; θ_e is electrical angle of mover, and satisfies $\theta_e = \pi x / \tau_s$; $\pi/2$ is added since q -axis component is with a 90 degree phase lead.

Substituting (8) and (9) into (7), and Supposing the desired thrust is F_x^* , it yields the following formula

$$\frac{3\pi}{2\tau_s} \left(\sum_{k=0}^{+\infty} \Psi_{d\pm 6k} e^{i\left(\pm 6k\frac{\pi x}{\tau_s}\right)} \right) \cdot \left(i_0 + \sum_{k=1}^{+\infty} i_{\pm 6k} e^{i\left(\pm 6k\pi\theta_e + \frac{\pi}{2}\right)} \right) + \sum_{k=1}^{+\infty} F_{c\pm 6k} e^{i\left(\pm 6k\frac{\pi x}{\tau_s}\right)} = F_x^* \quad (11)$$

Numerous linear equations can be derived from above expression and thrust ripple of any order can be eliminated in theory if the number and amplitude of current harmonics are not limited. However, the bandwidth of controller is limited in reality, it will cause large error when tracking reference currents of high frequency. Meanwhile, too many currents harmonics also increase the burden of controller. Since the 6th harmonic thrust accounts for the biggest part of thrust ripple [5], only 6th current harmonics are needed to suppress the 6th harmonic thrust ripple. In this case, equation (11) can be expressed as

$$\frac{3\pi}{2\tau_s} \left(\Psi_{d0} + \Psi_{d-6} e^{-j6\frac{\pi x}{\tau_s}} + \Psi_{d6} e^{j6\frac{\pi x}{\tau_s}} \right) \cdot \left(i_{q0} + i_{-6} e^{-j6\frac{\pi x}{\tau_s}} + i_{6} e^{j6\frac{\pi x}{\tau_s}} \right) + F_{c-6} + F_{c6} = F_x^* \quad (12)$$

By combining the same order harmonic terms, it yields the following equation

$$\frac{3\pi}{2\tau_s} \begin{bmatrix} \Psi_{d0} & i_{-6}\Psi_{d6} & i_{6}\Psi_{d-6} \\ i_{-6}\Psi_{d-6} & \Psi_{d0} & 0 \\ i_{6}\Psi_{d6} & 0 & \Psi_{d0} \end{bmatrix} \begin{bmatrix} i_{q0} \\ i_{-6} \\ i_{6} \end{bmatrix} = \begin{bmatrix} F_x^* \\ -F_{c-6} \\ -F_{c6} \end{bmatrix} \quad (13)$$

From (13), the amplitude of desired q -axis current can be solved. Here the 12th electromagnetic force harmonic equations are neglected, since the force generated by harmonic current and flux harmonic is relatively small and will make the equation has no solution.

B. Multiple rotating Reference Frames

PI controllers are applied in traditional RFOC of LSLSM as d, q axes current controller. Restricted by bandwidth, it is difficult for PI controller to track ± 6 th harmonics reference current in d, q coordinate, especially at high speed. However, these harmonics in d, q coordinate can be converted to dc component in the coordinate rotating at the same frequency of harmonic. In this case, the synchronous reference frames rotating at multiple times the speed of

d, q coordinate are introduced and stator currents with different frequencies are controlled independently. The ± 6 th reference harmonic current in d, q coordinate corresponds to 7th and 5th harmonic in stationary reference frame, respectively. The multiple reference frames introduced in this paper are depicted as diagram below.

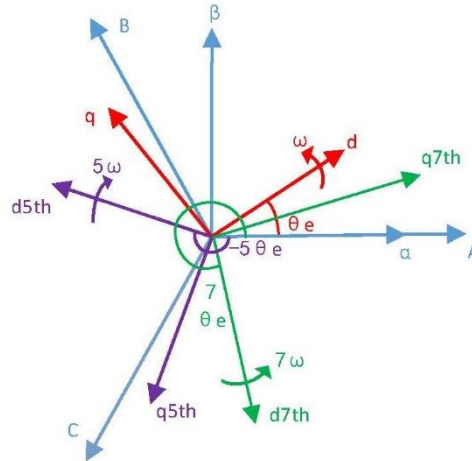


Fig. 1. The multiple reference frames of LSLSM, where A, B, C and α, β are the stationary reference frame; d, q coordinate rotate synchronously with mover, and $\omega = \pi\nu/\tau_s$ is the synchronous speed corresponding to electric angular speed of mover; $d5, q5th$ coordinate rotate at 5 times the speed of d, q coordinate reversely; $d7, q7th$ coordinate rotate at 7 times the speed of d, q coordinate in the same direction

The transformation matrix from α, β coordinate to multiple rotating reference frames can be expressed as

$$T(k\theta_e) = \begin{bmatrix} \cos(k\theta_e) & \sin(k\theta_e) \\ -\sin(k\theta_e) & \cos(k\theta_e) \end{bmatrix} \quad (14)$$

where $k = 1, -5, 7, \dots$

After coordinate transformation, current components with same angular speed with reference frame become constant, while others are alternating. Then the dc component can be abstracted after a low-pass filter, which is the magnitude of real current harmonic. Thus, the closed-loop feedback control of current harmonics can be established as shown below

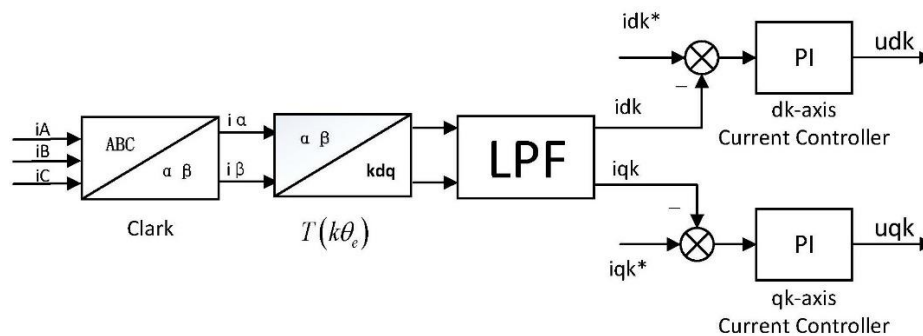


Fig. 2. The diagram of harmonic current closed-loop feedback control,

where idk^* and iqk^* are the reference values of k th harmonics current in k th reference frame,

and satisfy

$$\begin{cases} id5^* + i \cdot iq5^* = i_{-6} \\ id7^* + i \cdot iq7^* = i_6 \end{cases} \quad (15)$$

C. Harmonic Voltage Decouple and Feedforward Control

In conventional d, q axes current controller, the d, q axes currents are decoupled by compensation of EMF, the voltage equation in the d, q axes after compensation of EMF can be written as

$$\begin{cases} u_d^* = u_d + \frac{\pi}{\tau_s} v \Psi_q = R_s i_d + L_d \frac{di_d}{dt} \\ u_q^* = u_q - \frac{\pi}{\tau_s} v \Psi_d = R_s i_q + L_q \frac{di_q}{dt} \end{cases} \quad (16)$$

where u_d^* and u_q^* are d, q axes voltage generated by current PI controllers respectively.

Substitute (15) into (11), the desired current in d, q coordinate can be rewritten as

$$\begin{cases} i_{d5}^1 = i_{d5} \cos(-6\omega t) - i_{q5} \sin(-6\omega t) \\ i_{q5}^1 = i_{d5} \sin(-6\omega t) + i_{q5} \cos(-6\omega t) \\ i_{d7}^1 = i_{d7} \cos(6\omega t) - i_{q7} \sin(6\omega t) \\ i_{q7}^1 = i_{d7} \sin(6\omega t) + i_{q7} \cos(6\omega t) \end{cases} \quad (17)$$

where i_{d5}^1 and i_{q5}^1 are the voltage of 5th current harmonic in d, q coordinate; i_{d7}^1 and i_{q7}^1 are the voltage of 7th current harmonic in d, q coordinate.

Since the inductance L_d and L_q are approximately equal in LSLSM, $L = L_d = L_q$ is introduced to simplify the equation. By substituting (17) into (16), the harmonic voltage equations can be written as

$$\begin{cases} u_{d5}^1 = R_s i_{d5}^1 + 6\omega L i_{q5}^1 \\ u_{q5}^1 = R_s i_{q5}^1 - 6\omega L i_{d5}^1 \\ u_{d7}^1 = R_s i_{d7}^1 - 6\omega L i_{q7}^1 \\ u_{q7}^1 = R_s i_{q7}^1 + 6\omega L i_{d7}^1 \end{cases} \quad (18)$$

where u_{d5}^1 and u_{q5}^1 are the voltage of 5th current harmonic in d, q coordinate; u_{d7}^1 and u_{q7}^1 are the voltage of 7th current harmonic in d, q coordinate.

By rotating coordinate transformation of the voltage equations in d, q coordinate, the voltage equations of 5th current harmonic in $d5, q5$ coordinate can

be expressed as

$$\begin{cases} u_{d5}^5 = R_s i_{d5} + 6\omega L i_{q5} \\ u_{q5}^5 = R_s i_{q5} - 6\omega L i_{d5} \end{cases} \quad (19)$$

Similarly, the voltage equations of 7th current harmonic in $d7, q7$ coordinate can be expressed as

$$\begin{cases} u_{d7}^7 = R_s i_{d7} - 6\omega L i_{q7} \\ u_{q7}^7 = R_s i_{q7} + 6\omega L i_{d7} \end{cases} \quad (20)$$

To increase the response speed of harmonics, the voltage feedforward is introduced. The feedforward voltage can be calculated according to reference currents and voltage equations, that is

$$\begin{cases} u_{d5_com} = R_s i_{d5}^* + 6\omega L i_{q5}^* \\ u_{q5_com} = R_s i_{q5}^* - 6\omega L i_{d5}^* \\ u_{d7_com} = R_s i_{d7}^* - 6\omega L i_{q7}^* \\ u_{q7_com} = R_s i_{q7}^* + 6\omega L i_{d7}^* \end{cases} \quad (21)$$

where $u_{i_com}, i = d5, q5, d7, q7$ are the feedforward voltages on $d5, q5$ axes and $d7, q7$ axes, respectively.

From harmonic voltage equations in (19) and (20), it can be seen the currents in dk, qk axes are coupled. Thus, the decoupled harmonic current controllers with voltage feedforward are designed. The following diagram shows the structure of 5th current harmonic controller.

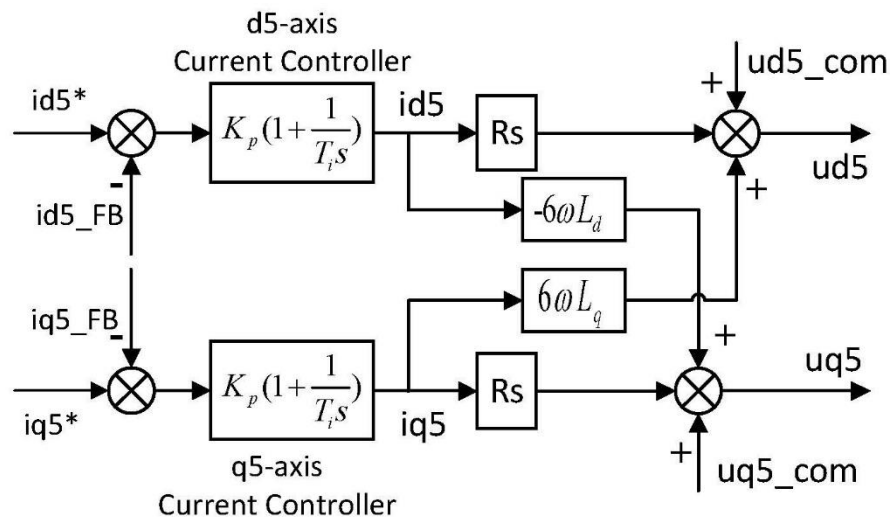


Fig. 3. The diagram of 5th harmonic current closed-loop feedback control,

where errors of harmonic current are sent to PI controller, whose output is also current. The final output of harmonic current controller is harmonic voltage, made up by feedback control voltage and feedforward steady state voltage.

The controller of 7th current harmonic can be designed in the same way according to (19) and (21).

SIMULATION AND RESULTS

The performance of the proposed thrust ripple suppression method for LSLSM has been tested through simulation experiments on MATLAB/Simulink. The LSLSM applied in simulation is one stator section of 960 m long with one maglev frame. The maglev frame of equal pole pitch is built in Maxwell software as shown in Fig. 4.

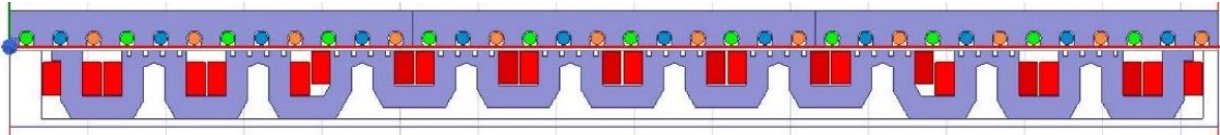


Fig. 4. Simulation model of LSLSM in Maxwell of equal pole pitch

Through finite element calculation, not only the parameters of maglev frame, but also the flux linkage with fluctuation and cogging force are obtained, considering non-linear properties of LSM. From that, the 6th harmonics of flux linkage and cogging force are obtained by Fourier transformation, and considered in the LSLSM simulation model. The main parameters of LSLSM are listed in Table 1, where the parameters of stator are based on the maglev test line.

Table 1. Parameters of LSLSM

Parameter	Value	Parameter	Value
Stator resistance (Ω)	0.2237	Excitation flux (wb)	0.1171
Stator inductance L_d (mH)	2.4817	Pole pitch (mm)	266.5
Stator inductance L_q (mH)	2.4764	Mass (kg)	3000

The block diagram of the thrust controlled LSLSM drive system is depicted in Fig. 5. Here only current closed loop control is included instead of position-speed-current control because it's enough to validate the effect of thrust ripple suppression. The LSLSM is fed by three level neutral point clamped voltage source inverter, whose rated voltage is 1900 V and rated current is 1200 A. The switching frequency of inverter and control frequency of current controller are 2 kHz. At first, the optimal reference current are determined by the current assignment block based on equation (13) and (15). The stator currents of different frequency are controlled independently in multiple reference frames. By coordinate transformations and low-pass filters, the feedback of current in multiple rotating reference frames are obtained from the measured stator current. The controller of current on d, q axes is a decoupled PI controller with voltage compensation for EMF. The 5th and 7th current harmonics are controlled by decoupled PI controllers with steady state voltage feedforward

on $d5, q5$ and $d7, q7$ coordinate, respectively. Finally, the control voltage of each current controller are transformed to α, β stationary reference frame, and together make up the voltage reference u_{α}^* and u_{β}^* of SVPWM, which generates gate signals of inverter.

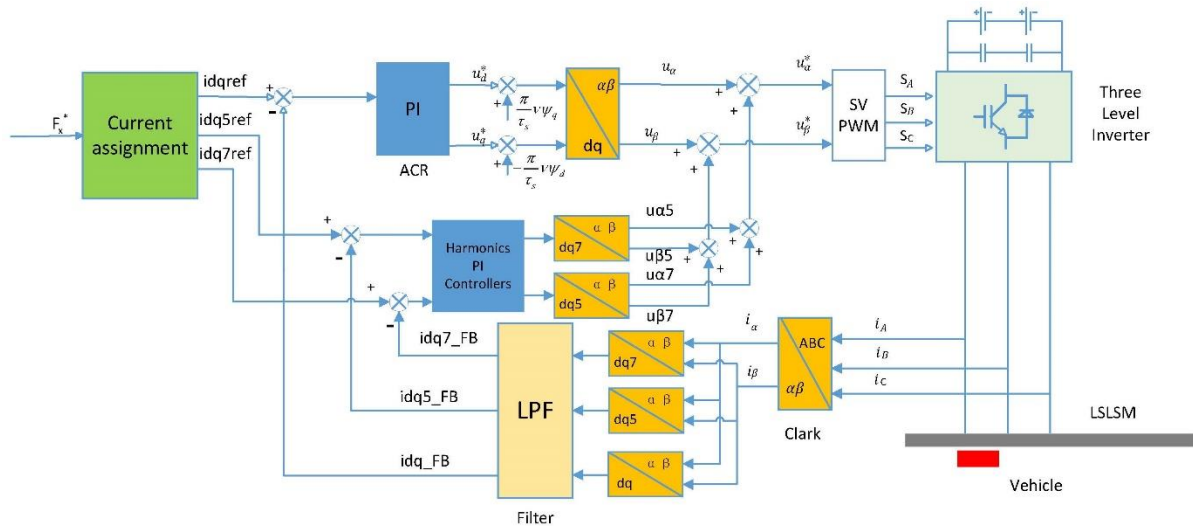


Fig. 5. The block diagram of thrust controlled drive system for LSLSM

In Fig. 6–8, results of one simulation test are shown. In this test, the thrust ripple of without harmonic current injection, harmonic current injection by proposed harmonic current controller and injection by conventional PI current controller are compared. From 0–1s, no harmonic current is injected into stator current. The proposed thrust ripple suppression strategy is applied at 1.0 s. From 2.0 s to the end, the injected harmonic current is controlled only by PI controllers on d, q axes. The load force is 1500 N and the maglev frame is propelled to 10.66 m/s and corresponding fundamental frequency of stator current is 20 Hz.

Fig. 6 shows the waveforms of thrust force. There are severe 6th thrust ripple before 1.0 s. The magnitude of thrust ripple is about 150 N, approximately to the cogging force. After applying the proposed harmonic current injection method, the thrust ripple is reduced significantly. But conventional PI controller can't control harmonic currents well, as the thrust ripple is nearly reduced after 2.0 s. The thrust waveforms during switching algorithm period are shown in Fig. 6 (b) and 6 (c). Fig. 6(b) shows the proposed algorithm can suppress thrust ripple very fast.

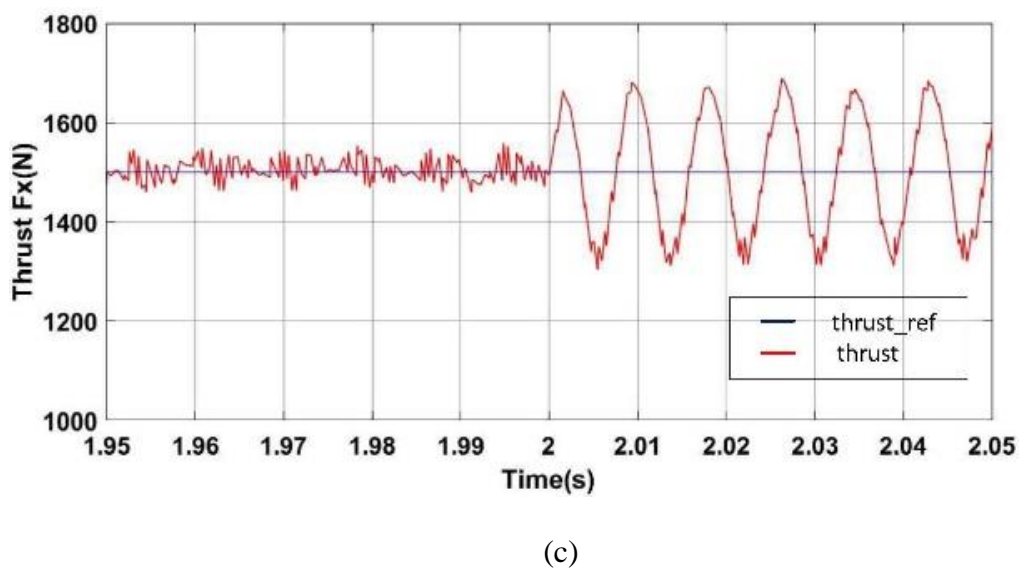
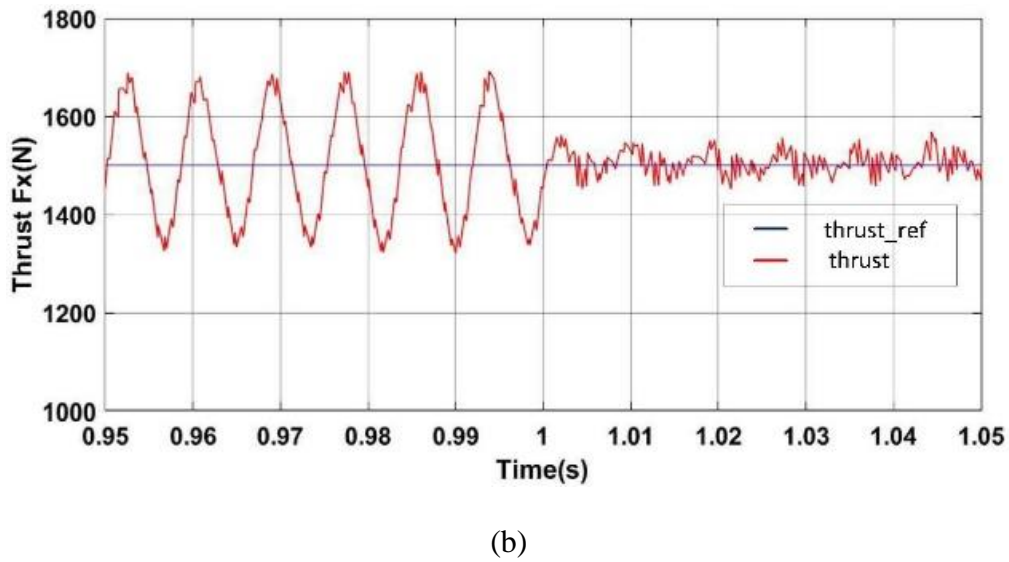
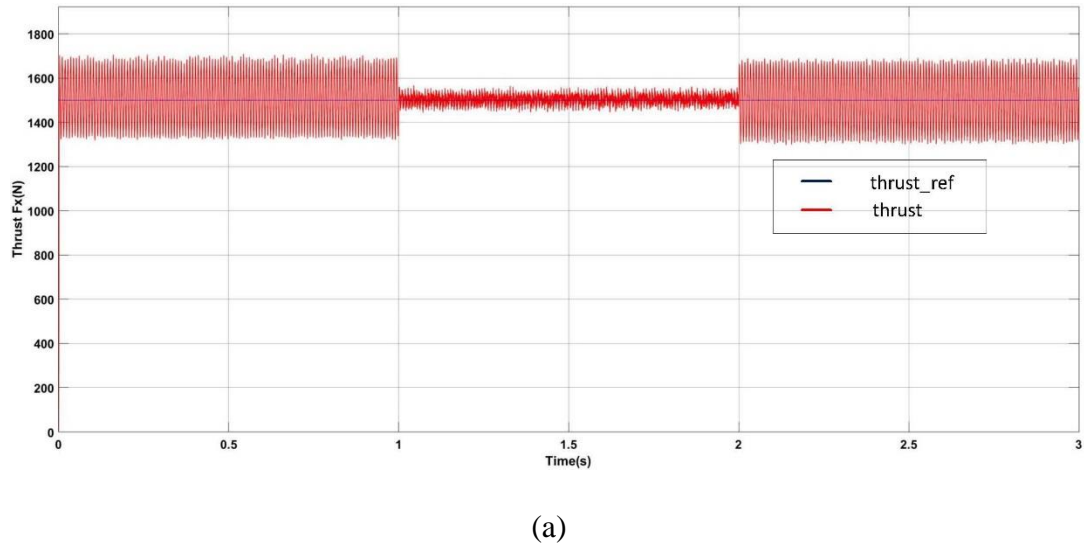


Fig. 6. The thrust waveforms of LSLSM

Spectrum analysis of thrust at 0.7 s, 1.7 s and 2.7 s are shown in Fig. 7 (a–c), respectively. The original magnitude of 6th thrust ripple is 10.38 % of the average thrust, about 155 N. After injection of harmonic current, the magnitude of 6th thrust ripple is reduced to 0.41 % of the average thrust, about 7 N. Meanwhile, the magnitude of 12th thrust ripple remains almost the same. It shows good effect of the proposed thrust ripple suspension method. It can be seen from Fig. 7(c) the harmonic current injection by current loop on d, q axes can't reduce thrust ripple but slightly increase it.

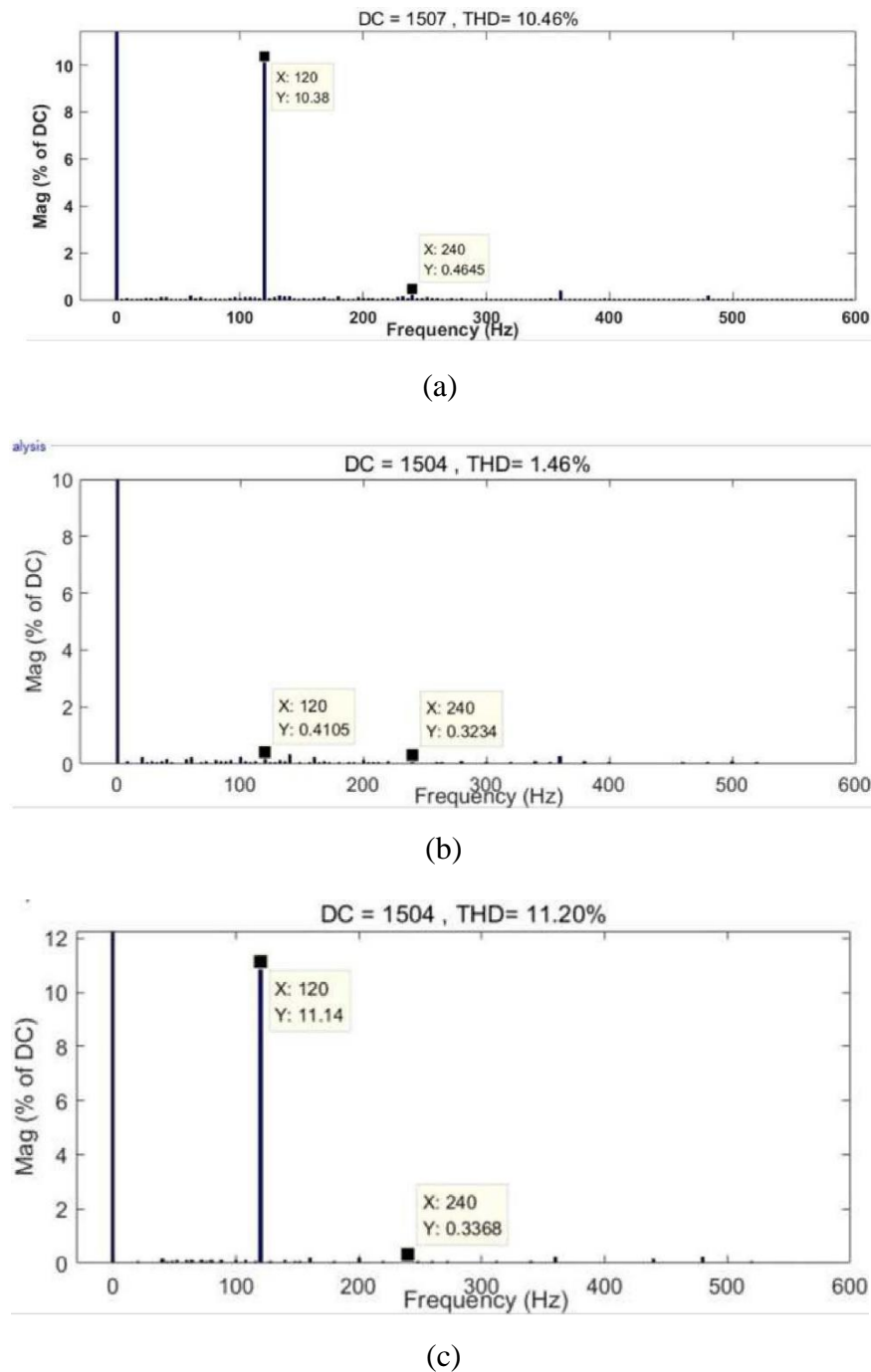


Fig. 7. The Spectrum diagram of thrust force at different times

The response of the currents on d, q axes are shown in Fig. 8. The current waveforms during switching algorithm are shown in Fig. 8(b) and 8(c). It can be seen current harmonics are injected into q -axis current after 1.0 s in Fig. 8(a). The waveform in Fig. 8(b) shows that the real currents can follow the reference values accurately and quickly, which validate the effectiveness of the proposed harmonic current controller. From Fig. 8(c), it can be seen there are large phase delay between reference harmonic current and feedback. That's why harmonic current injection by conventional PI current controller are not able to suppress thrust ripple well.

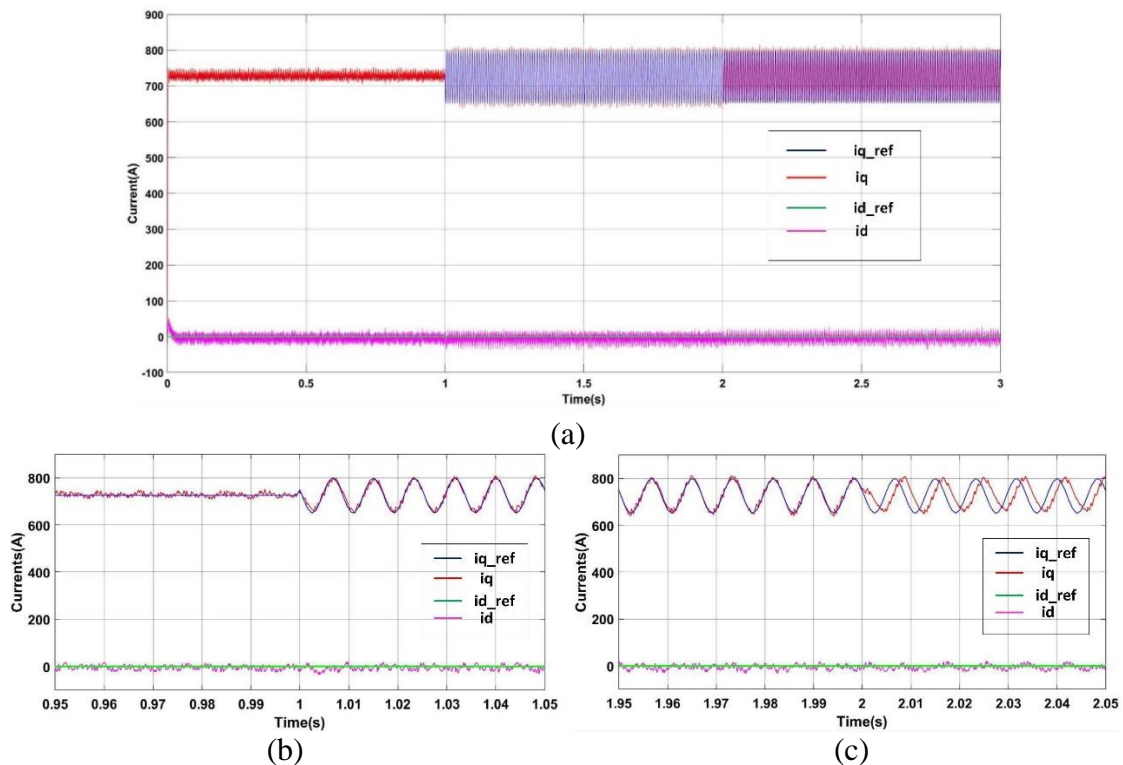


Fig. 8. The waveforms of stator current on d, q axes

CONCLUSION

A thrust ripple suppression method by harmonic current injection is presented in this paper. The LSLSM model considering flux linkage harmonics and cogging force is established, which are the main sources of thrust ripple. The flux linkage harmonics and cogging force are calculated by finite element method in Maxwell software. Harmonic current injection is proposed to generate harmonic electromagnetic force of opposite phase. The method to determine proper stator current is derived. The adequate stator current is made up by fundamental and 5th and 7th harmonics, which can suppress the main 6th thrust ripple of LSLSM effectively. Then, multiple rotating reference frames are introduced, since the alternating current and voltage become constant values in

the corresponding rotating coordinate. Harmonic currents are controlled independently in their synchronous rotating reference coordinate, which decoupled the control of fundamental and harmonic current, and overcome the bandwidth limitation of PI controller on d, q axes current. At last, the voltage model of harmonic current is studied. Based on the voltage equations, the decoupled harmonic current controllers are designed. The steady state voltage feedforward of harmonics current is applied, which increase response speed of harmonics current. Simulation test results validate the proposed scheme can suppress the 6th thrust ripple of LSLSM effectively and quickly.

ACKNOWLEDGEMENTS

This work was supported by the National Key Technology R&D Program of China (2016YFB1200602-02).

References

1. Lu G, Cheng H, He W, Zhang J, Pan G. Harmonic analysis of the PWM inverter fed LSM drive system. In the TRANSRAPID Shanghai. Proceedings of the 6th International Conference in Advances in Power System Control, Operation and Management, 2003. p. 547–557. doi: 10.1049/cp:20030646
2. Wang M, Li L, Yang R. Overview of thrust ripple suppression technique for linear motors. *Chinese Journal of Electrical Engineering*. 2017;2(1):77-84. Available at: <https://ieeexplore.ieee.org/document/7933117/>. doi: 10.23919/CJEE.2016.7933117
3. Ma M, Li L, Zhang J, Yu J, Zhang H, Jin Y. Analytical Methods for Minimizing Detent Force in Long-Stator PM Linear Motor Including Longitudinal End Effects. *IEEE Transactions on Magnetics*, 2015;51(11):1-4. doi: 10.1109/intmag.2015.7156725
4. Zhu YW, Lee SG, Chung KS, Cho YH. Investigation of Auxiliary Poles Design Criteria on Reduction of End Effect of Detent Force for PMLSM. *IEEE Transactions on Magnetics*. 2009;45(6):2863-2866. doi: 10.1109/tmag.2009.2018778
5. Yang G, Wang K, Zhang Z. Study on electromagnetic force ripple reduction of long stator linear synchronous motor based on unequal pole pitch. Proceedings of the International Conference on Electrical Machines and Systems. 2017. p. 1-4. doi: 10.1109/icems.2017.8055994
6. Hwang SH, Kim JM. Dead Time Compensation Method for Voltage-Fed PWM Inverter. *IEEE Transactions on Energy Conversion*, 2010;25(1):1-10. doi: 10.1109/tec.2009.2031811
7. Liao Y, Zhen S, LIU R, Yao J. Torque Ripple Suppression of Permanent Magnet Synchronous Motor by the Harmonic Injection. *Proceeding of the CSEE*, 2011;31(21):119-127. Available at: <http://www.pcsee.org/CN/Y2011/V31/I21/119#>.
8. Zhao S, Tan KK. Adaptive feedforward compensation of force ripples in linear motors. *Control Engineering Practice*, 2005;13(9):1081-1092. doi: 10.1016/j.conengprac.2004.11.004
9. Cho K, Kim J, Park H, Choi SB. Periodic adaptive disturbance observer for a Permanent Magnet Linear Synchronous Motor. Proceedings of the 51st IEEE Conference on Decision and Control (CDC), 2012. p. 4684–4689. doi: 10.1109/cdc.2012.6426591

10. Chen SL, Hsieh TH. Repetitive control design and implementation for linear motor machine tool. *International Journal of Machine Tools & Manufacture*, 2007;47(12):1807-1816. doi: 10.1016/j.ijmachtools.2007.04.009
11. Yan Y, Li W, Deng W, Zhang G, Xia C. Torque ripple minimization of PMSM using PI type iterative learning control. Proceedings of the IECON 2014 40th Annual Conference of the IEEE; 2014; IEEE; 2015. p. 925-931. doi: 10.1109/iecon.2014.7048612
12. Xu S, Zhao W, Ji J, Du Y, Zhang D, Liu G. Thrust ripple reduction of linear flux-switching PM motor using harmonic injected current. Proceedings of the International Conference on Electrical Machines and Systems; IEEE; 2014. p. 1886-1889. doi: 10.1109/icems.2013.6713220
13. Guan B, Zhao Y, Yi R. Torque Ripple Minimization in Interior PM Machines using FEM and Multiple Reference Frames. Proceedings of the Conference on Industrial Electronics and Applications; 2006; IEEE;2006. p. 1-6. doi: 10.1109/iciea.2006.257208
14. Shang KJ, Chen X, Zhou Y. A Harmonic Voltage and Current Coupling Permanent Magnet Synchronous Motor Model and Feedforward Control. *Transactions of China Electrotechnical Society*, 2017;32(18):131-142. Available at: <http://www.ces-transaction.com//CN/Y2017/V32/I18/131>. doi: 10.19595/j.cnki.1000-6753.tces.161956
15. Ge Q, Li Y, Kong L. A comparative study of FOC for long stator linear synchronous motor control. Proceedings of the International Conference on Electrical Machines and Systems (ICEMS); 2007; IEEE; 2007. p. 398-402. Available at: <https://ieeexplore.ieee.org/abstract/document/4411996/>.
16. Wang X, Liu H, Zhang S. High performance propulsion control of magnetic levitation vehicle long stator linear synchronous motor. Proceedings of the International Conference on Electrical Machines and Systems; 2011; IEEE, 2011. p. 1-6. doi: 10.1109/icems.2011.6073798.

Information about the authors:

Jinsong Kang, PhD, professor; Tongji University; No.4800, Cao An Road, Shanghai, China.
ORCID: 0000-0003-4875-1818;

E-mail: kjs@tongji.edu.cn

Siyuan Mu, Bachelor of science, PhD candidate;

ORCID: 0000-0002-3006-1301;

E-mail: siyuanmu@tongji.edu.cn

Shuo Wang, Master of science, PhD candidate;

ORCID: 0000-0003-3123-3942;

E-mail: 1988wangshuo@tongji.edu.cn

Yusong Liu, Bachelor of science, PhD candidate;

ORCID: 0000-0002-0520-389X;

E-mail: liuyusong@tongji.edu.cn

Cuiwei He, Master of science, Master;

E-mail: hcw1964@163.com

To cite this article:

Mu S, Kang J, Wang S, et al. A method of thrust ripple suppression for long stator linear synchronous motor. *Transportation Systems and Technology*. 2018;4(2):30-44. doi: 10.17816/transsyst20184230-44